Observed variability of water properties and transports on the World Ocean Circulation Experiment SR1b section across the Antarctic Circumpolar Current

Marc A. García,[1,2] Ileana Bladé,[1] Antonio Cruzado,[3] Zoila Velásquez,[3] Hernán García,[4] Joan Puigdefàbregas,[1] and Joaquim Sospedra[1]

Received 15 February 2000; revised 3 May 2001; accepted 13 September 2001; published 18 October 2002.

[1] R/V *Hespérides* occupied the World Ocean Circulation Experiment SR1b repeat section across the Scotia Sea in February 1995, February 1996, and February 1998. On each cruise the same set of 21 hydrographic stations with characteristic spacing <20 nautical miles was visited. The results of the three surveys display a characteristic zonation of water masses in the region, which is defined by four hydrographic fronts. The net geostrophic transport of the Antarctic Circumpolar Current (ACC) across SR1b, computed with reference to the deepest common depth of each pair of adjacent stations, is similar in all three cruises, 144 Sv in February 1995, 131 Sv in February 1996, and 134 Sv in February 1998, and compares well with earlier computations of the ACC transport across Drake Passage. A close comparison of the vertical distributions of water properties on SR1b reveals changes in the structure of the ACC that are linked to undersampled current mesoscale activity, as suggested by infrared satellite images contemporary to the cruises. The most remarkable features are several ''hydrographic discontinuities'' observed in the Antarctic Zone south of the Southern ACC Front (SACCF), which are believed to be signatures of eddies produced east of the Shackleton Fracture Zone. The paper further addresses the different contribution of each ACC zonal band to the net geostrophic transport across SR1b on each *Hespérides* occupation. *INDEX TERMS:* 4512 Oceanography: Physical: Currents; 4528 Oceanography: Physical: Fronts and jets; 4532 Oceanography: Physical: General circulation; *KEYWORDS:* WOCE, Southern Ocean, Antarctic Circumpolar Current, water masses, fronts, transports

Citation: García, M. A., I. Bladé, A. Cruzado, Z. Velásquez, H. García, J. Puigdefàbregas, and J. Sospedra, Observed variability of water properties and transports on the World Ocean Circulation Experiment SR1b section across the Antarctic Circumpolar Current, *J. Geophys. Res.*, *107*(C10), 3162, doi:10.1029/2000JC000277, 2002.

1. Introduction

[2] World Ocean Circulation Experiment (WOCE) Core Project 2 (CP2) was designed to quantify the contribution of the Southern Ocean to the world climate. The specific goals of CP2 were to assess the Antarctic Circumpolar Current (ACC) transport and the current's dynamical balance, to quantify the meridional fluxes across the Southern Ocean and the exchanges between the Southern Ocean and the neighboring ocean basins, and to compute the atmosphere-ocean fluxes at the Southern Ocean surface [*World Meteorological Organization*, 1988]. One approach to these goals involved repeated hydrographic sampling at selected ACC choke points during the WOCE field phase. One of the targeted repeat sections was SR1b, extending between Burdwood Bank and Elephant Island, east of Drake Passage (Figure 1). At the request of the CP2 Scientific Steering Group and as a part of the Spanish contribution to WOCE, R/V *Hespérides* covered the WOCE SR1b section in February 1995 and in February 1996. A third occupation of SR1b was carried out by *Hespérides* during the Deep Ocean Ventilation through Antarctic Intermediate Layers (DOVETAIL) project in February 1998, shortly after completion of the WOCE data acquisition phase. This paper discusses, beyond the preliminary reports by *García* [1996] and *García et al.* [1997], the variability of water properties and transports on SR1b as observed during the above mentioned *Hespérides* cruises. Parallel data sets were obtained by R/V *James Clark Ross* during a series of SR1b repeats initiated in November 1993 [*King and Alderson*, 1994], which were staggered in time relative to the *Hespérides* occupations. This complementarity between the U.K. and the Spanish field efforts on SR1b should be beneficial for the WOCE data integration phase.

[1]Laboratori d'Enginyeria Marítima, E.T.S. d'Enginyers de Camins, Canals i Ports, Universitat Politècnica de Catalunya, Barcelona, Spain.
[2]Now at Direcció General de Ports i Transports, Generalitat de Catalunya, Barcelona, Spain.
[3]Centre d'Estudis Avançats de Blanes, Consejo Superior de Investigaciones Científicas, Blanes (Girona), Spain.
[4]Scripps Institution of Oceanography, University of California, San Diego, La Jolla, California, USA.

0148-0227/02/2000JC000277$09.00

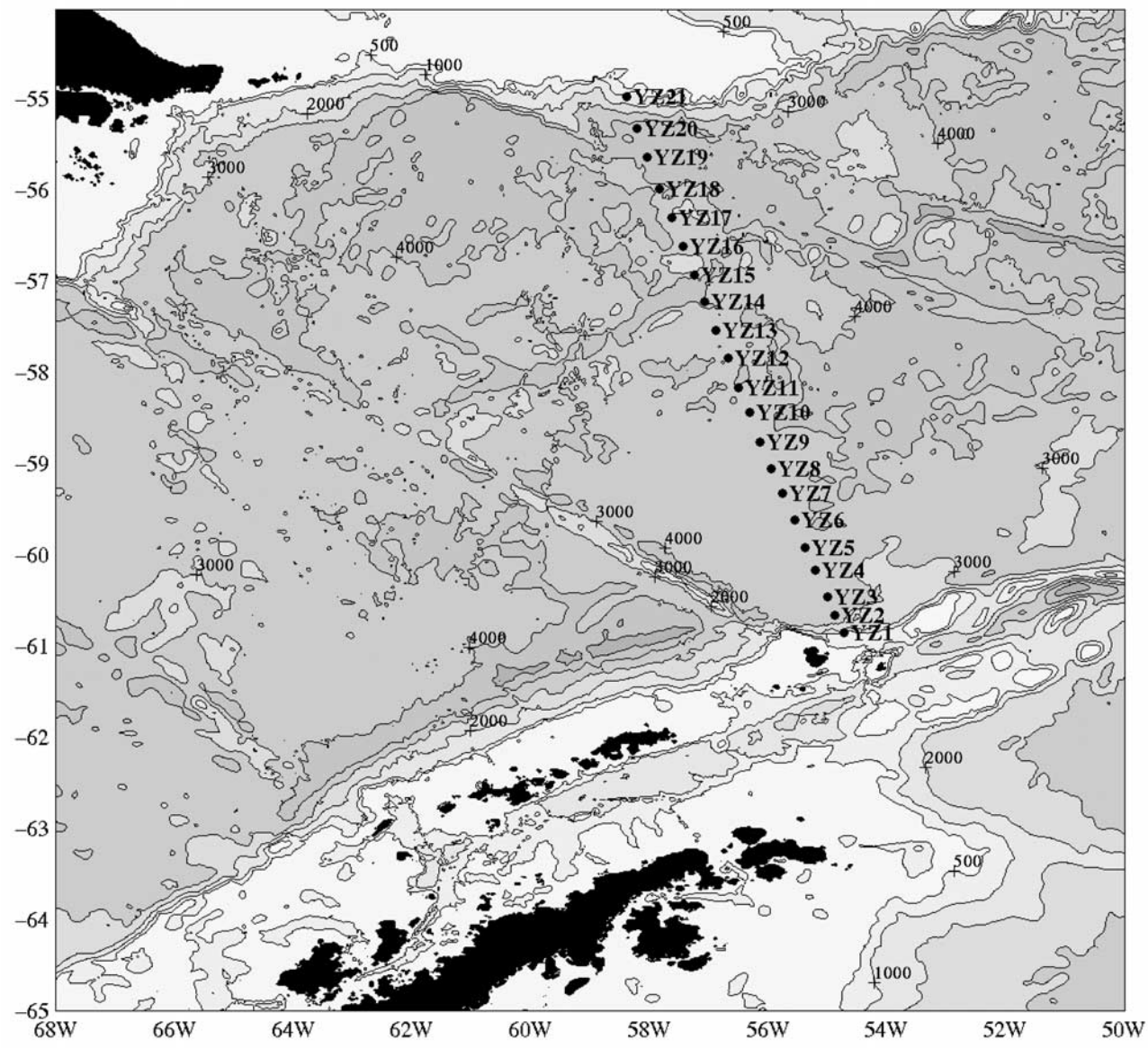

Figure 1. Location of the WOCE SR1b section and stations occupied by R/V *Hespérides* during the Drake 95, Drake 96, and Drake 98 cruises. The underlying bathymetry is from *Smith and Sandwell* [1997].

[3] The structure of the paper is straightforward. In section 2 the equipment and the methods used during the *Hespérides* cruises and in further data postprocessing are described. A presentation of the vertical distributions of water properties on SR1b and of computed geostrophic current velocities across the section follows. Next, the zonation and frontal structure of the ACC is discussed in relation to the water mass and geostrophic flow distributions, including several mesoscale structures observed in the southern Antarctic Zone. The ACC transport variability is also discussed. The legacy of papers produced under the umbrella of the U.S. International Southern Ocean Study (ISOS) Program [e.g., *Whitworth*, 1983; *Whitworth and Peterson*, 1985] and several other recent studies addressing the ACC zonation [*Orsi et al.*, 1995] and the variability of the ACC hydrography and transport [*Moore et al.*, 1997; *Challenor et al.*, 1996; *Meredith et al.*, 1996] are the main references for the discussion. A wrap-up summary and conclusion section closes the paper.

2. Material and Methods

[4] R/V *Hespérides* occupied the WOCE SR1b section across the Scotia Sea on 15–20 February 1995 (Drake 95 cruise), on 15–20 February 1996 (Drake 96 cruise), and again on 13–18 February 1998 (DOVETAIL cruise, hereinafter referred to as Drake 98). On each survey the same set of 21 hydrographic stations with characteristic spacing of <20 nautical miles was visited (Figure 1). At every station, surface-to-bottom conductivity-temperature-depth (CTD) casts were performed with a General Oceanics (GO) MkIIIC WOCE CTD probe (an MkV in Drake 98) equipped with temperature, salinity, dissolved oxygen, fluorescence, and light transmission sensors. Discrete water samples were obtained at 24 levels with a GO 1014 Rosette

carrying 12 L Niskin bottles, following WOCE procedures. Some of the bottles ported reversible thermometers. All water samples were analyzed onboard during the cruises. Water properties calculated from samples were salinity (with a Guildline 8600 A Autosal), dissolved oxygen (Winkler method following *Carpenter* [1965]), and dissolved inorganic nutrients (nitrate, nitrite, ortophosphate, and ortosilicate with a Skalar autoanalyzer, after *Whitledge et al.* [1981]). CTD temperature and salinity data from the Drake 95 and Drake 96 cruises were postprocessed and postcalibrated following WOCE standard methods [*WOCE*, 1998]. As for the Drake 98 CTD data, an equivalent postprocessing/postcalibration method was applied but for a reduced number of Autosal data per station. CTD dissolved oxygen, fluorescence, and light transmission data were not postcalibrated. Consequently, oxygen and nutrient distributions shown in this paper are derived from water sample data.

[5] Acoustic Doppler current profiler (ADCP) velocity profiles were obtained with a vessel-mounted RD Instruments 150 kHz narrowband system (the Skyfix stations located in the Falkland Islands and in Buenos Aires were used for Differential GPS (DGPS) positioning). However, during the Drake 96 and Drake 98 surveys the reception of the DGPS signal onboard *Hespérides* was frequently interrupted. Therefore only the Drake 95 ADCP data set will be used here. The ADCP data were postprocessed following routine methods to extract 2 km averaged current profiles. The transducer misalignment was corrected following *Joyce* [1989] and *Pollard and Read* [1989], and ADCP calibration exercises were carried out over Burdwood Bank. No tidal correction was applied to the data.

[6] A spatial objective interpolation scheme (objective mapping) has been used to interpolate potential temperature θ and salinity S sections from pressure-averaged CTD profiles. The detailed 0–500 dbar θ and S distributions in Figures 2 and 3 have been derived from 10 dbar averaged profiles, whereas 50 dbar averaged data have been used to build full depth sections (Figures 2, 3, and 4). The selected objective interpolation length scales are 50 km in the horizontal and 50 m in the vertical (200 m for full depth sections). A cruder linear interpolation between adjacent 50 dbar averaged profiles has been chosen to display potential density and cross-section geostrophic velocity distributions without masking any noteworthy dynamical features. Property distributions from water sample data (oxygen, nutrients, and chlorophyll) have been plotted using the Surface Mapping System contouring package from Golden Software Inc. Different vertical scales have been used to interpolate those fields between 0 and 1000 dbar and at levels below 1000 dbar.

3. Results

[7] Figures 2 and 3 display the observed distributions of potential temperature and salinity on SR1b during all three Drake cruises. Figure 4 shows the potential density section for Drake 95. The two fronts that characterize the classical zonation of the ACC, the Subantarctic Front (SAF) and the Polar Front (PF), can be easily traced in the temperature field (Figure 2). The location of the SAF can be deduced from the steepness of the 3°–5°C isotherms, which is maximum at this ACC front, and by the rapid northward sinking of the salinity minimum associated with the Antarctic Intermediate Water (AAIW) [*Whitworth and Nowlin*, 1987]. Following *Orsi et al.* [1995], we consider that the core of the SAF was located at the latitude where the 4°C isotherm intersected the 400 m layer, so between stations YZ18 and YZ19 (i.e., ~55.8°S) during Drake 95 and Drake 96 and between stations YZ16 and YZ17 (~56.5°S) in Drake 98. On the other hand, the PF is defined hydrographically as the northern boundary of the Antarctic Surface Water (AASW), which is characterized in summer by a subsurface temperature minimum embedded in an intense halocline [*Peterson and Stramma*, 1991]. According to the criterion originally proposed by *Deacon* [1933] and further systematized by *Orsi et al.* [1995], the PF was located where the temperature minimum was sinking below the 200 m depth, so between stations YZ13 and YZ14 (~57.4°S) in Drake 95 and Drake 98 and between stations YZ14 and YZ15 (~57.1°S) in Drake 96.

[8] *Orsi et al.* [1995] provided conclusive evidence of an additional, deep-reaching ACC front located south of the PF, which they named Southern ACC Front (SACCF). The SACCF can best be traced through the isopycnal tilt affecting the whole water column (Figure 4), but *Orsi et al.* [1995] showed that its position can also be identified on meridional potential temperature sections as the latitude at which the deep θ_{max} exceeds 1.8°C to the north at depths >500 m. Following this rule of thumb and cross checking it with the potential density distributions, we conclude that the SACCF was located approximately between stations YZ8 and YZ9 (~58.9°S) during Drake 95 and Drake 96 and between stations YZ10 and YZ11 (~58.3°S) during Drake 98.

[9] The southern boundary of the ACC (hereinafter referred to as southern ACC Bdy) was defined by *Orsi et al.* [1995] as the locus where the Upper Circumpolar Deep Water entrains the mixed layer and is lost in θ-S space. In the older literature the southern ACC Bdy at Drake Passage was often named Continental Water Boundary or Scotia Front. We may use *Orsi et al.*'s [1995] recipes for the identification of the southern ACC Bdy to trace its position on SR1b and, in particular, their criterion for the temperature field: a decrease of potential temperature below 0°C on σ_0 = 27.6 kg m^{-3}. With this convention the southern ACC Bdy turned out to be between stations YZ1 and YZ2 (~60.8°S) in Drake 95 and Drake 98 and south of YZ1 (i.e., south of 60.9°S) in Drake 96.

[10] North of the SAF, AAIW is found. It is usually characterized by a deep (below 400 m) salinity minimum, but at Drake Passage this minimum is not very well defined. In our three cruises the AAIW can be identified as an intermediate layer of water with nearly uniform salinity between 34.15 and 34.2 psu. Above this AAIW lies Subantarctic Surface Water with temperature values exceeding 7°C and surface minimum salinity values under 34.1 psu (Figures 2 and 3). Below the AAIW layer a two-layer Circumpolar Deep Water body is found. The deep salinity maximum (S up to 34.72 psu) is hosted by the Lower Circumpolar Deep Water (LCDW) layer; the shallower Upper Circumpolar Deep Water (UCDW) layer is warmer [*Reid and Lynn*, 1971; *Callahan*, 1972]. At this location, however (i.e., north of the SAF), no clear dis-

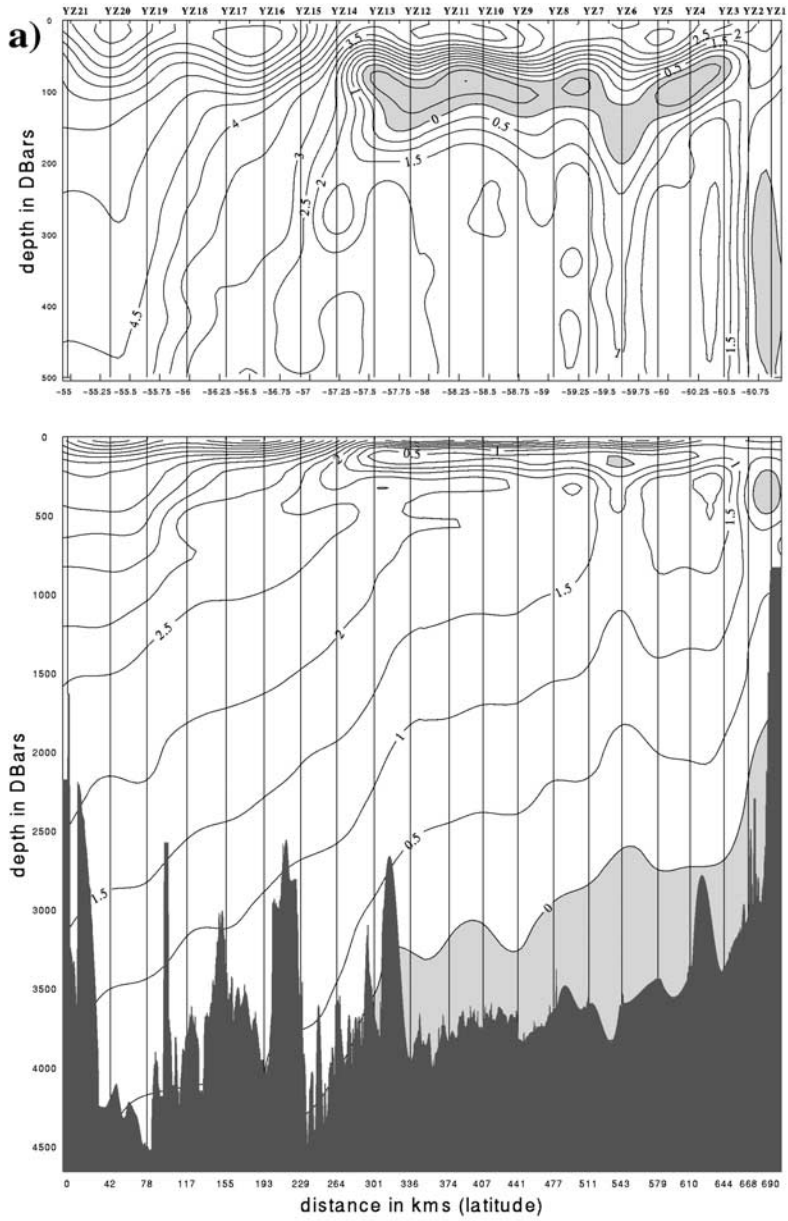

Figure 2. Potential temperature distributions (0–500 dbar and full depth sections) on SR1b during (a) Drake 95, (b) Drake 96, and (c) Drake 98. Burdwood Bank is on the left. Units are degrees Celsius, and contour interval is 0.5°C. Light (dark) shading indicates temperatures above (below) 1.5°C (0°C).

tinction between UCDW and LCDW can be made on the basis of θ and *S* alone. The core of the UCDW layer is best traced as a southward rising deep oxygen minimum (O_2 < 180 μmol kg^{-1}) and deep nitrate and phosphate maximum ($NO_3 + NO_2 > 34$ μmol kg^{-1} and $PO_4 > 2.4$ μmol kg^{-1}), as seen in Figure 5. Farther south, between the SAF and the southern ACC Bdy, the UCDW layer can be identified by a distinct deep temperature maximum (above 1°C), which, like the LCDW salinity maximum, rises toward the south. The UCDW then vanishes north of the southern ACC Bdy, having become entrained to the mixed layer [*Orsi et al.*, 1995].

[11] AAIW is lost south of the PF. In this region, colder and fresher AASW is found overlying the UCDW layer. Since all the Drake surveys were conducted during Austral summer, the temperature minimum of the AASW core (θ < 0°C) shows up in our temperature distributions as a subsurface feature underlying a warm skin layer (see Figure 2). On the other hand, the lowest salinity values associated with AASW were always obtained at the surface (*S* < 34.0 psu; Figure 3). Also south of the PF, we observe negative potential temperatures below LCDW. This is the signature of the Weddell Sea Deep Water (WSDW) outflow into the Scotia Sea, which flows westward and spreads northward along the northern slope of the South Shetlands archipelago. The northernmost extent of WSDW (i.e., the locus where the 0°C potential isotherm intersects the ocean bottom) appears to have progressively retreated poleward from

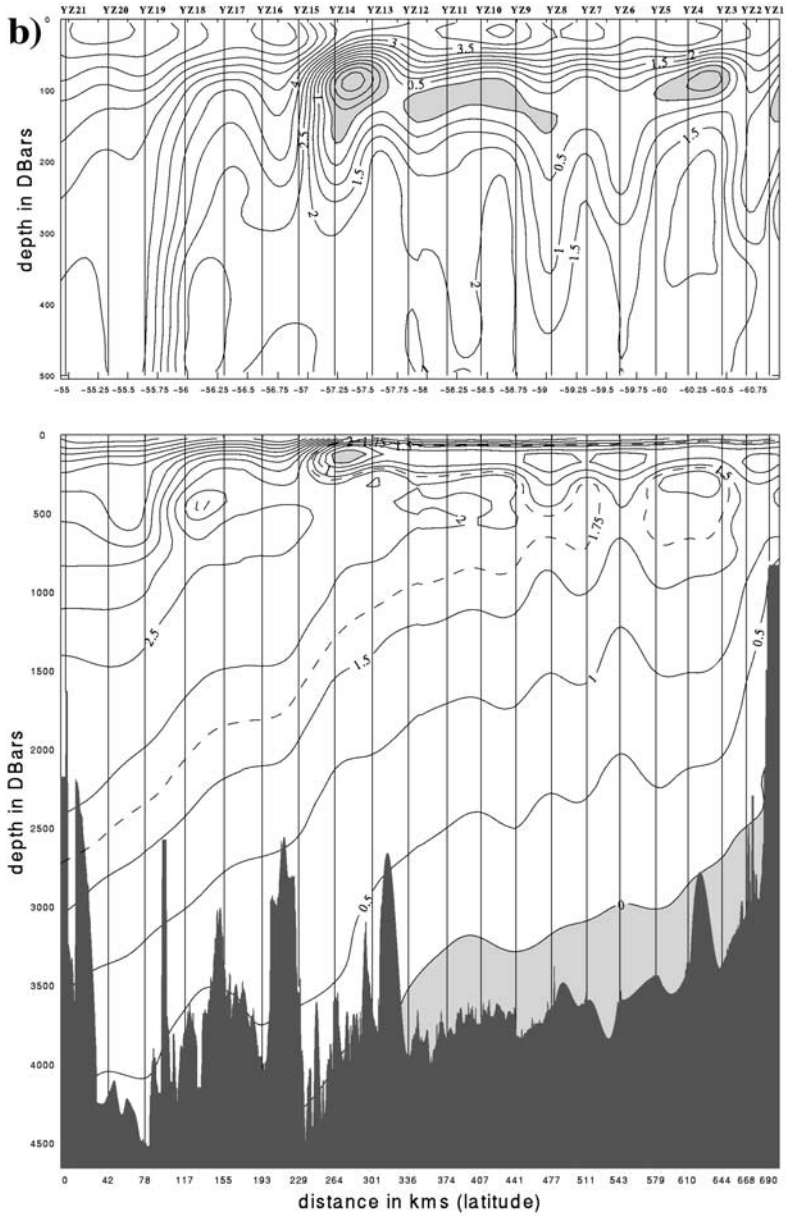

Figure 2. (continued)

1995 to 1998. This is also suggested by the changes observed in the O_2 distribution from one occupation to the other (Figure 5).

[12] No surface changes were observed across the SACCF on any of the SR1b occupations. This is consistent with *Orsi et al.* [1995], who noted that the SACCF is the only ACC front that does not separate distinct surface water masses as the AASW layer extends all the way from the Antarctic continental shelf to the PF. On the other hand, our water property distributions display prominent discontinuities (''jumps'') in the UCDW layer south of the SACCF. In Drake 95 we clearly observe such a discontinuity in the temperature, salinity, and dissolved oxygen fields at station YZ6 (Figures 2, 3, and 5). We also notice a very similar discontinuity in the Drake 98 distributions of θ and oxygen at station YZ8 (Figures 2 and 3). In Drake 96 we observe a similar, if weaker, feature again at YZ6.

[13] Figure 6 displays the distribution of geostrophic velocities and transports across SR1b during Drake 95, Drake 96, and Drake 98. The maximum common depth between adjacent stations has been used as the zero-motion reference layer; the current velocity has been assumed to be zero in the ''triangles'' below the near-bottom reference level. The Drake 95 results (Figure 6a) display a four-jet current distribution across the section that is related to the frontal structure described above. The maximum computed geostrophic velocities (~50 cm s^{-1}) are obtained within the SAF jet at the surface. The PF jet displays slightly lower velocities of up to about 45 cm s^{-1} but is wider and thus makes a greater contribution to the total ACC transport (Table 1). The jet associated with the SACCF is much

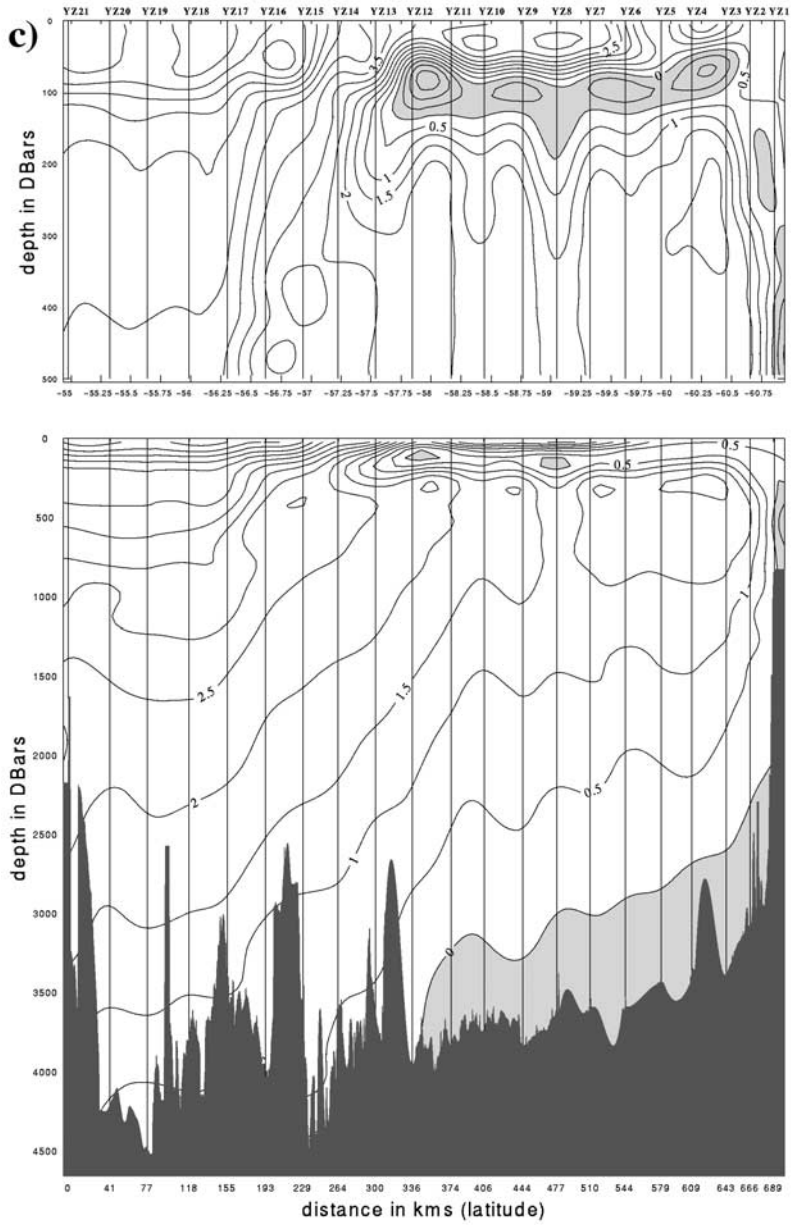

Figure 2. (continued)

weaker, with maximum geostrophic velocities under 15 cm s^{-1}. Bands of weak reversed (i.e., westward) geostrophic flow are found at both the northern and southern flanks of the SACCF jet. A fourth jet related to the southern ACC Bdy with maximum velocities of about 20 cm s^{-1} at 300 m depth is found on the South Shetlands slope. The Drake 96 situation is qualitatively similar to the February 1995 picture but with several noteworthy differences (Figure 6b). The SAF jet is at the same latitude but is much more intense and achieves maximum geostrophic velocities of about 70 cm s^{-1} at the surface. A westward flowing band is found north of the SAF jet. The PF jet appears split into two branches, a main one sitting some 20 nm (1 station) north of its position in February 1995 and having maximum geostrophic velocities of up to 50 cm s^{-1} and a second one located about 20 nm south, with maximum velocities slightly over 20 cm s^{-1}. The SACCF current band also appears as a jet split into two veins. As for the jet related to the southern ACC Bdy, it shows up again as a slope current but with somewhat weaker maximum velocities (about 10 cm s^{-1}) than in Drake 95. The Drake 98 geostrophic flow distribution (Figure 6c) shows both a significant southward shift and an overlapping of the SAF and PF bands. The core of the SAF jet has maximum geostrophic velocities of about 65 cm s^{-1}, whereas the PF jet core displays values of up to 45 cm s^{-1}. The surface velocities in the region between both jets exceed 25 cm s^{-1}, so it is questionable whether we can actually distinguish a SAF and a PF current band. North of the SAF jet, a band of westward flow with maximum geostrophic velocities of up to 15 cm s^{-1} is found. South of the PF, there is another weaker westward flowing band separating it from the SACCF jet. As in Drake 96, the SACCF appears as a weaker

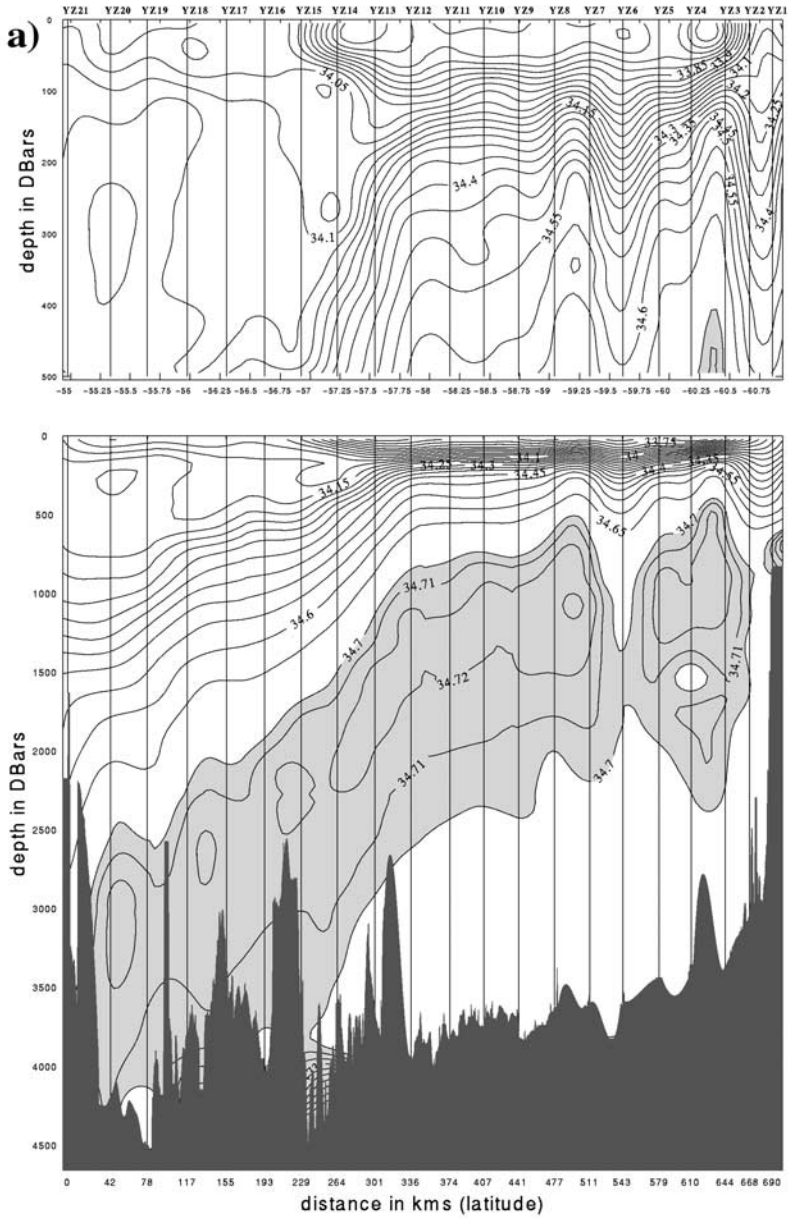

Figure 3. Salinity distributions (0–500 dbar and full depth sections) on SR1b during (a) Drake 95, (b) Drake 96, and (c) Drake 98. Burdwood Bank is on the left. Units are psu, and contour interval is 0.05 (0.01) psu below (above) 34.7 psu. Light (dark) shading indicates salinities below (above) 34.0 psu (34.7 psu).

jet (maximum velocities $\sim$10 cm s^{-1}) divided into two branches by a slow westward flowing band, and the southern ACC Bdy jet core is found on the northern slope of the South Shetlands archipelago with maximum geostrophic velocities of about 10 cm s^{-1}.

4. Discussion

4.1. ACC Zonation and Fronts at Drake Passage

[14] Over the past 2 decades, many authors have discussed the zonation of the ACC on the basis of water property and flow distributions [e.g., *Whitworth*, 1980; *Nowlin and Clifford*, 1982; *Deacon*, 1982; *Peterson and Stramma*, 1991]. More recently, *Orsi et al.* [1995] have proposed an objective classification of the ACC frontal zones based on all historical hydrographic data available for the Southern Ocean. An extremely valuable contribution of *Orsi et al.* [1995] has been the unambiguous hydrographic definition of the SACCF. This front had been identified in earlier papers [e.g., *Nowlin et al.*, 1977] but had not been described in a systematic manner.

[15] In *Orsi et al.*'s [1995] view the ACC is a three-front current system (SAF, PF, and SACCF) limited by a northern boundary (the Subtropical Front) and a southern boundary (the southern ACC Bdy). They propose to name the ACC's poleward edge simply "southern boundary of the ACC" rather than using the older "Continental Water Boundary" term, which is meaningful and well established only at Drake Passage. *Orsi et al.* [1995] noted in passing that at the Greenwich meridian the southern ACC Bdy appeared as a

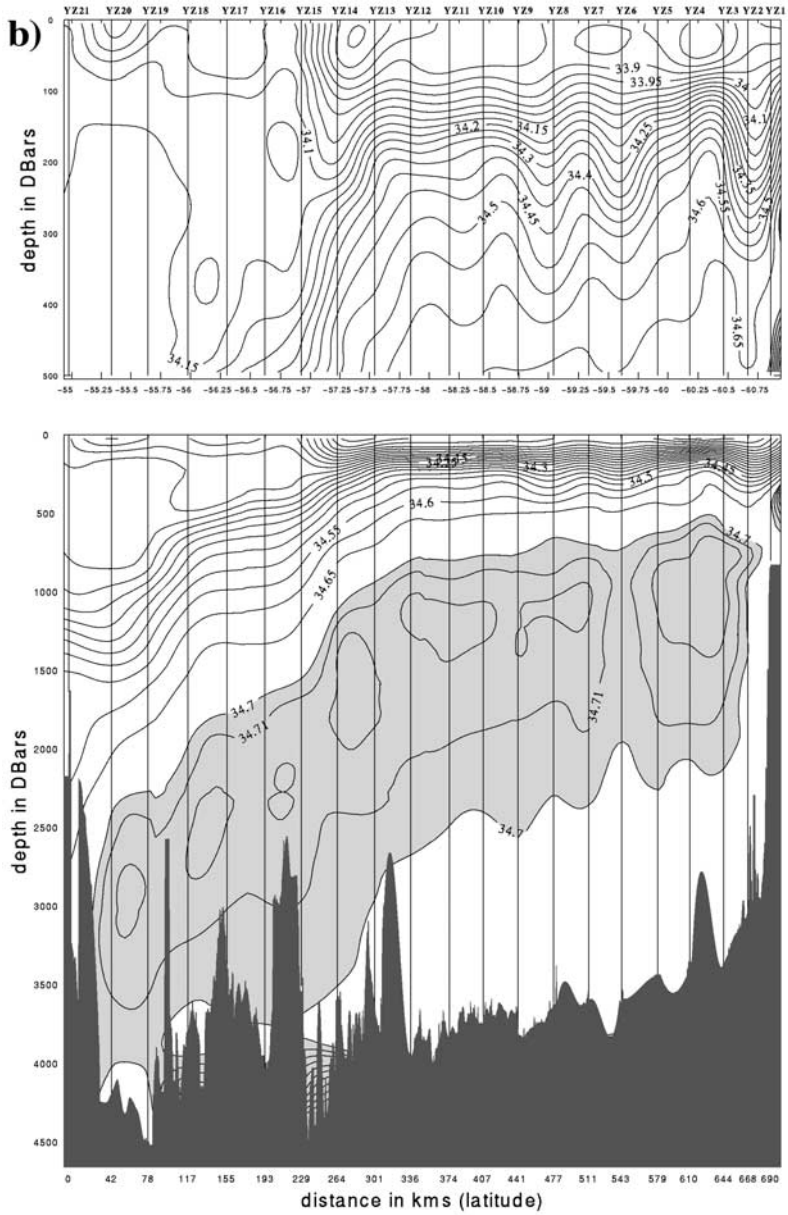

Figure 3. (continued)

region of enhanced geostrophic volume transport. Our results suggest that at SR1b, also, the southern ACC Bdy constitutes a permanent dynamical front since a baroclinic jet is associated with it in all three surveys. Therefore we may state that the ACC has a four-front structure on SR1b.

[16] The location of the ACC fronts during the *Hespérides* cruises, as identified using *Orsi et al.*'s [1995] recipes, is schematically depicted in Figure 7. For the February 1995 case these locations are in agreement with those initially reported by *García* [1996]; however, the February 1995 and February 1996 positions differ slightly from those given by *García et al.* [1997] because of the use of a coarser interpolation scheme in that other study (note that the SACCF was not discussed in that paper). It is interesting to compare the frontal locations assessed "hydrographically," i.e., on the basis of the vertical distributions of water properties in Figures 2, 3, and 4, with those resulting from applying an intuitive "dynamical" criterion to identify the position of a front, i.e., the latitude at which a relative maximum in the geostrophic velocity field is found. Figure 6 shows that by using this dynamical rule we obtain very similar positions for the four ACC fronts to those estimated following the hydrographic method. We therefore conclude that the hydrographic location criteria proposed by different authors and systematized by *Orsi et al.* [1995] are robust.

[17] The *Hespérides* data set illustrates some important changes in the position of the ACC fronts from one occupation to another. No obvious links, however, seem to exist between the excursions of the different fronts: comparing their positions in February 1996 with respect to February 1995, the SAF and the SACCF were at the same

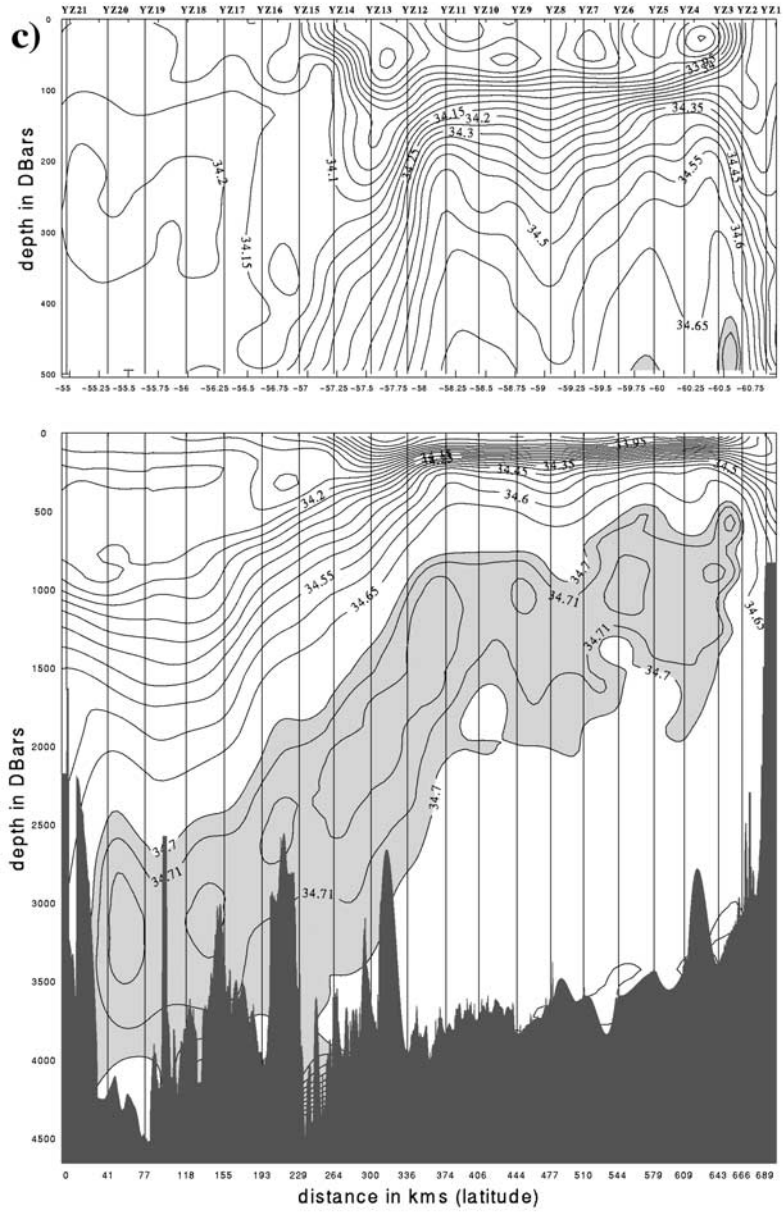

Figure 3. (continued)

latitude, the PF was farther north, and the southern ACC Bdy was farther south (Figure 7), whereas comparing the February 1998 locations with those observed in February 1996, the SAF and the PF were both farther south, but the SACCF and the southern ACC Bdy were both farther north. There is also no simple relationship between these excursions and the observed changes in the associated transports across SR1b (Table 1). For instance, one may have expected meridional excursions of a front to be accompanied by either lateral stretching or shrinking of the corresponding flow band or by increased or decreased tilt of isopycnals. Let us take the SAF case as an example. The front remained at the same latitude between February 1995 and February 1996, but the associated transport increased by 16 Sv, whereas the total ACC transport was reduced by 12 Sv (see Table 1). When the SAF "went south" in February 1998, however, the related transport was almost unchanged and so was the total ACC transport. Hence the results shown in Table 1 reflect the sum of many complex factors that influence the transport of the ACC across SR1b.

[18] In light of the results from monthly expendable bathythermograph (XBT) surveys across Drake Passage published by *Sprintall et al.* [1997] we are inclined to think that the frontal variability displayed by the *Hespérides* data is mainly the expression of undersampled mesoscale temporal variability. An inspection of *Sprintall et al.*'s [1997] temperature sections reveals meridional shifts of both the SAF and the PF from one month to the next that are of the same order of magnitude as the changes in position from Drake 95 to Drake 96 and from Drake 96 to Drake 98. This is also consistent with the range of the ACC transport

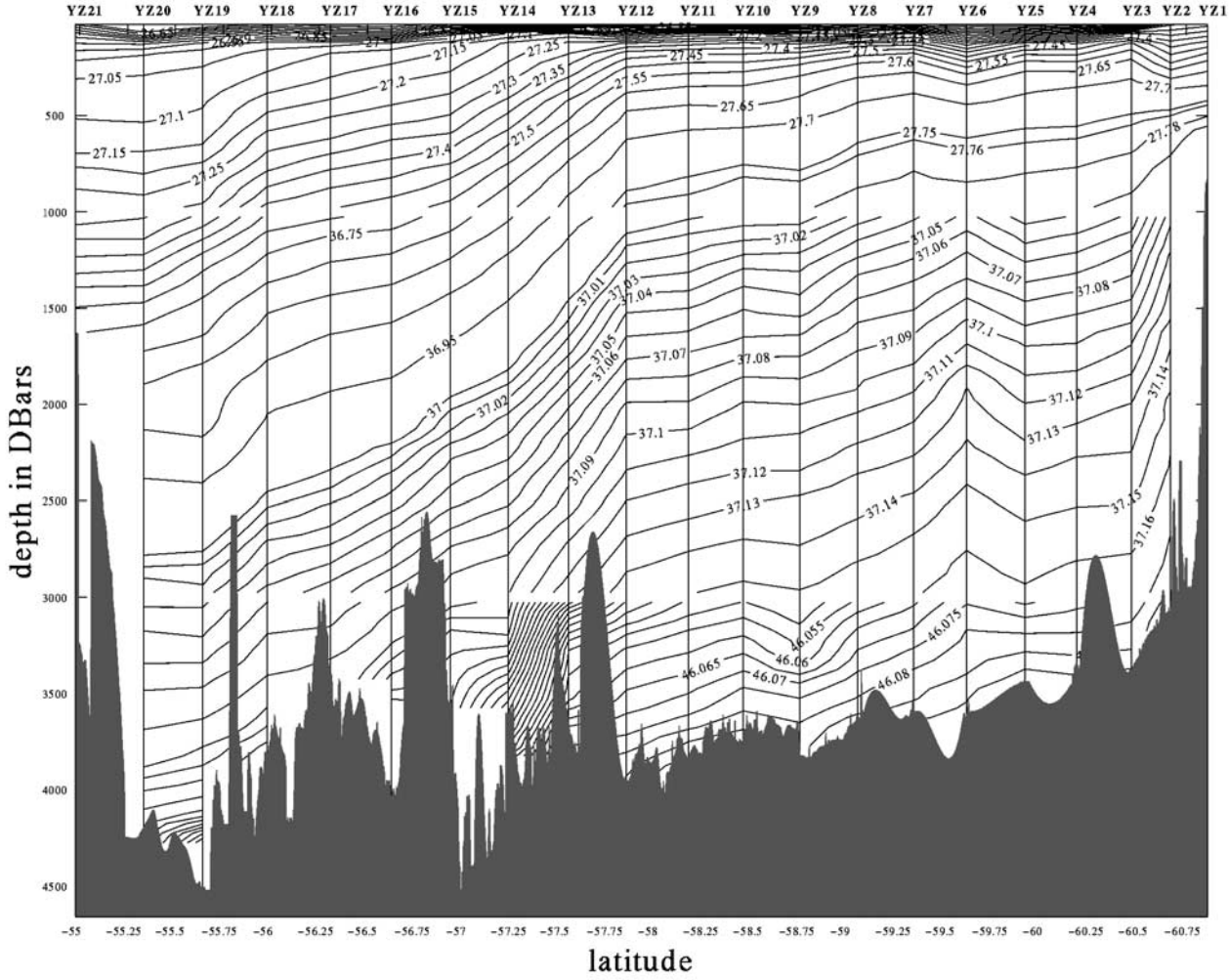

Figure 4. "Staggered" potential density (σ_0 between 0 and 1000 dbar, σ_2 between 1000 and 3000 dbar, and σ_4 below 3000 dbar) on SR1b during Drake 95. Burdwood Bank is on the left. Units are kg m^{-3}, and contour interval is variable.

mesoscale variability displayed by the ISOS time series [e.g., *Whitworth and Peterson*, 1985], which is of the same order of magnitude as the flow changes observed by us.

4.2. Mesoscale Variability in the Southern Antarctic Zone

[19] As noted above and by *García* [1996], the Drake 95 vertical distributions (Figures 2a and 3a) display an important "discontinuity" of water properties at station YZ6 (59.6°S), south of the SACCF, characterized by abnormally cold and fresh waters. This structure can be also discerned in the O_2 distribution but is not so evident in the nutrient sections (Figure 5). The Drake 96 distributions reveal a much less pronounced, though still noticeable, property discontinuity at the same station and perhaps also farther north, at station YZ8 (59.1°S; Figures 2b, 3b, and 5). Neither of them was well represented in the interpolated fields shown by *García et al.* [1997]. In Drake 98 a sharp discontinuity is again evident in temperature and dissolved oxygen and, somewhat less clearly, in salinity at station YZ8 (59.1°S) but not at station YZ6 (Figures 3c, 4c, and 5). A similar structure was observed during the November 1993 *James Clark Ross* cruise [*King and Alderson*, 1994] and has also been detected in subsequent British occupations of SR1b (B. King, personal communication, 1997). *King and Alderson* [1994] argued that the water column around which such a hydrographic discontinuity was evident in November 1993 consisted of [*King and Alderson*, 1994, p. 15] "relatively cold fresh water, apparently originating south of the Continental Water Boundary and found some 100 km out of place to the north." They considered this structure to be caused by an eddy but did not pursue this hypothesis any further. *Rojas et al.* [1998] reported on an occupation of SR1a (located some 250 nm west of SR1b) in December

Figure 5. (opposite) Vertical distribution of dissolved oxygen, nitrate plus nitrite, orthophosphate, and silicate on SR1b during (left) Drake 95, (middle) Drake 96, and (right) Drake 98. Burdwood Bank is on the left. Units are μmol kg^{-1}.

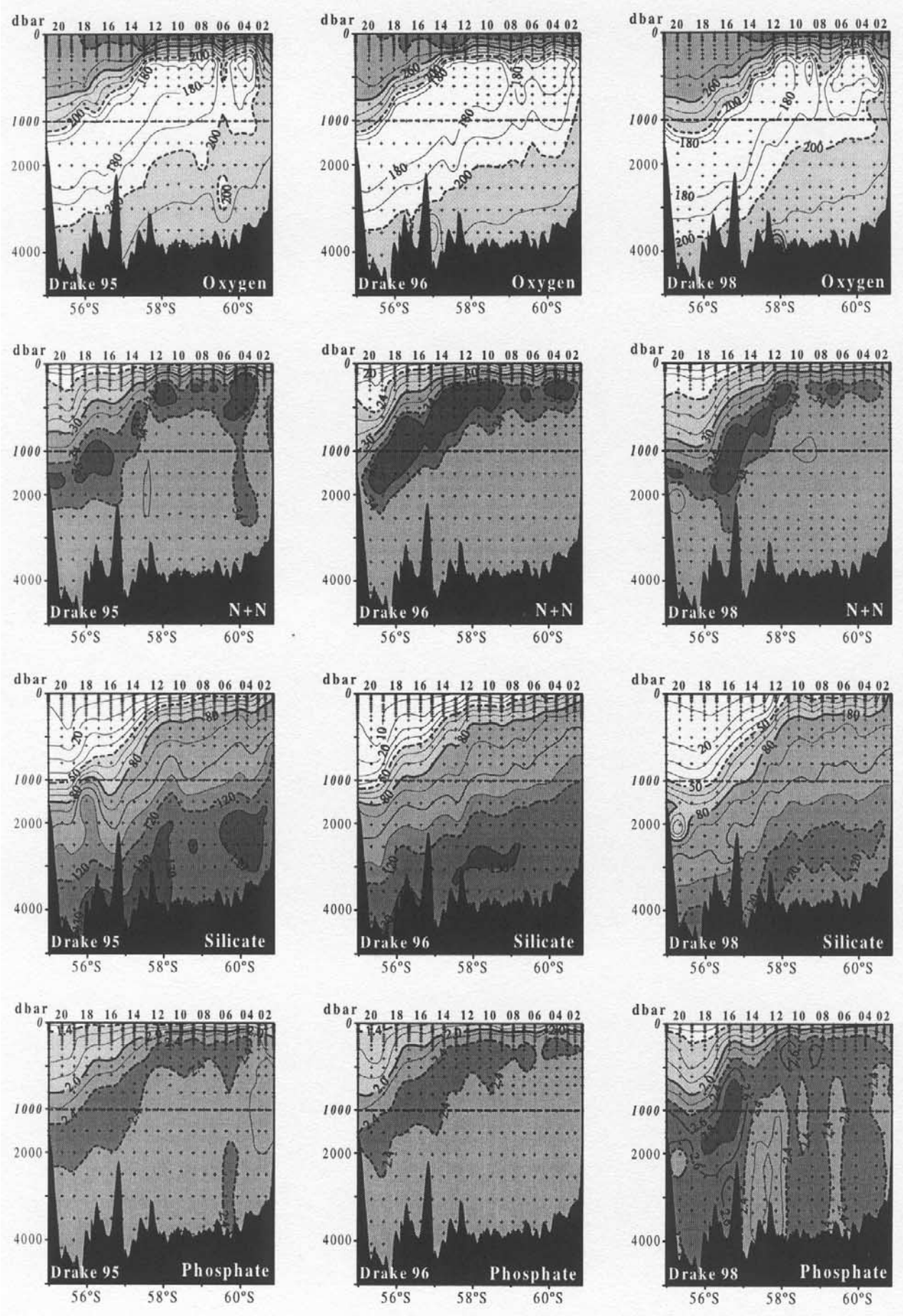
dbar
20 18 16 14 12 10 08 06 04 02
0
1000
2000
4000
Drake 95 Oxygen
Drake 96 Oxygen
Drake 98 Oxygen
Drake 95 N+N
Drake 96 N+N
Drake 98 N+N
Drake 95 Silicate
Drake 96 Silicate
Drake 98 Silicate
Drake 95 Phosphate
Drake 96 Phosphate
Drake 98 Phosphate
56°S
58°S
60°S

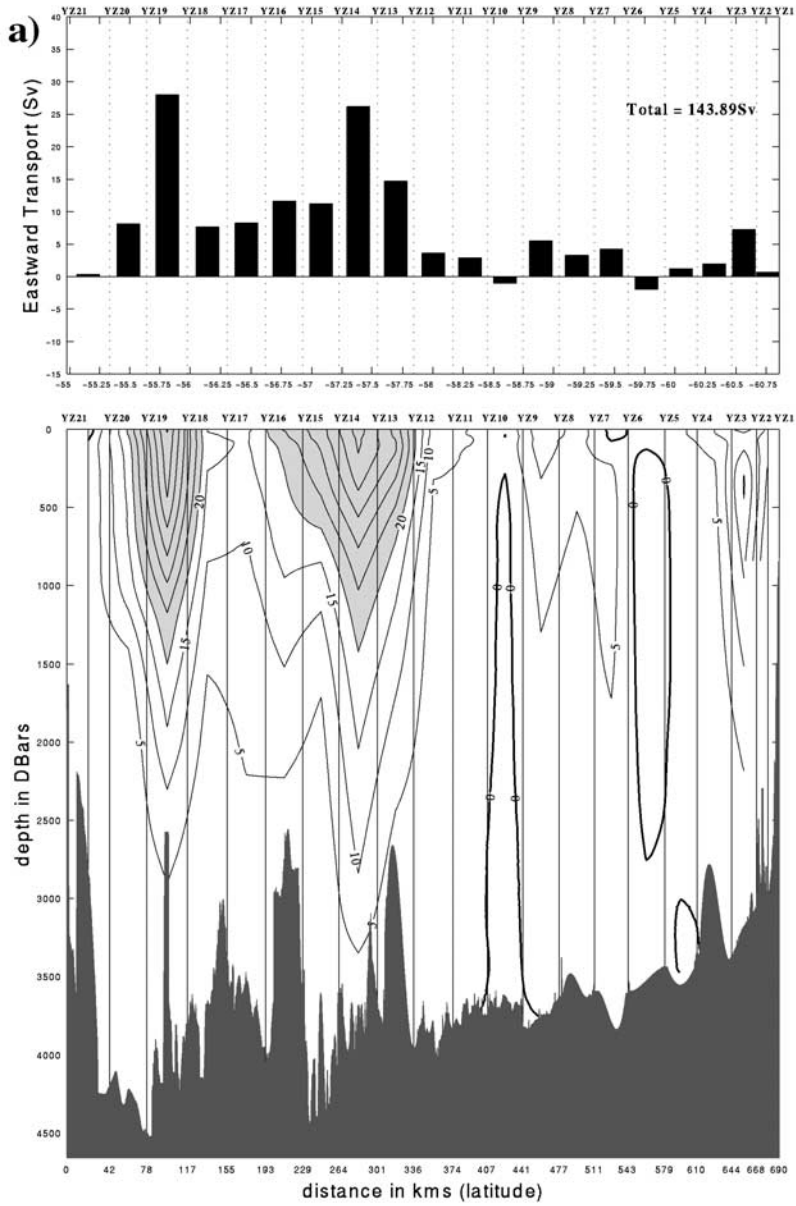

Figure 6. Geostrophic transports between pairs of stations (in Sv) and geostrophic current velocities across SR1b (in cm s^{-1}) during (a) Drake 95, (b) Drake 96, and (c) Drake 98. Burdwood Bank is on the left. The maximum common depth between adjacent stations has been used as the zero-motion reference layer.

1996; no hydrographic discontinuity is evident in their temperature and salinity sections.

[20] The question whether the previous discontinuities are related to eddies or are caused by current meanders deserves some further thought. Figure 8 displays the ADCP current distribution in the upper layer of SR1b during Drake 95. It shows that station YZ6 (~59.6°S), where a sharp hydrographic discontinuity (i.e., anomalously cold waters) is found, is flanked by a band of northeastward flow to the north and by a stretch of westward-northwestward flow to the south. The SACCF, located at 58.9°S, is north of that northeastward flowing band, and the northeastward jet related to the southern ACC Bdy is found immediately south of the westward current band. This westward current band is also evident in the geostrophic current field (Figure 6a) and is seen to occupy essentially the entire water column. This picture is consistent with a cyclonic eddy theory to explain the observed hydrographic anomaly, and geostrophy would support this interpretation (note the changing tilt of the deep isopycnals at 59.6°S in Figure 4a). However, alternative explanations could be proposed in view of Figures 2a, 3a, 5, and 8 if the stretch comprised between 59.6° and 60.7°S, and not the "chop" at 59.6°S, is considered to be the actual hydrographic anomaly, consisting of northern Antarctic Zone waters brought into the southern Antarctic Zone. One possible explanation is that the anomaly was due to a SACCF meander. This would mean we crossed the SACCF thrice in February 1995 and that the front's southernmost position was adjacent to the southern ACC Bdy, but this possibility does not seem likely to us. An alternative, and

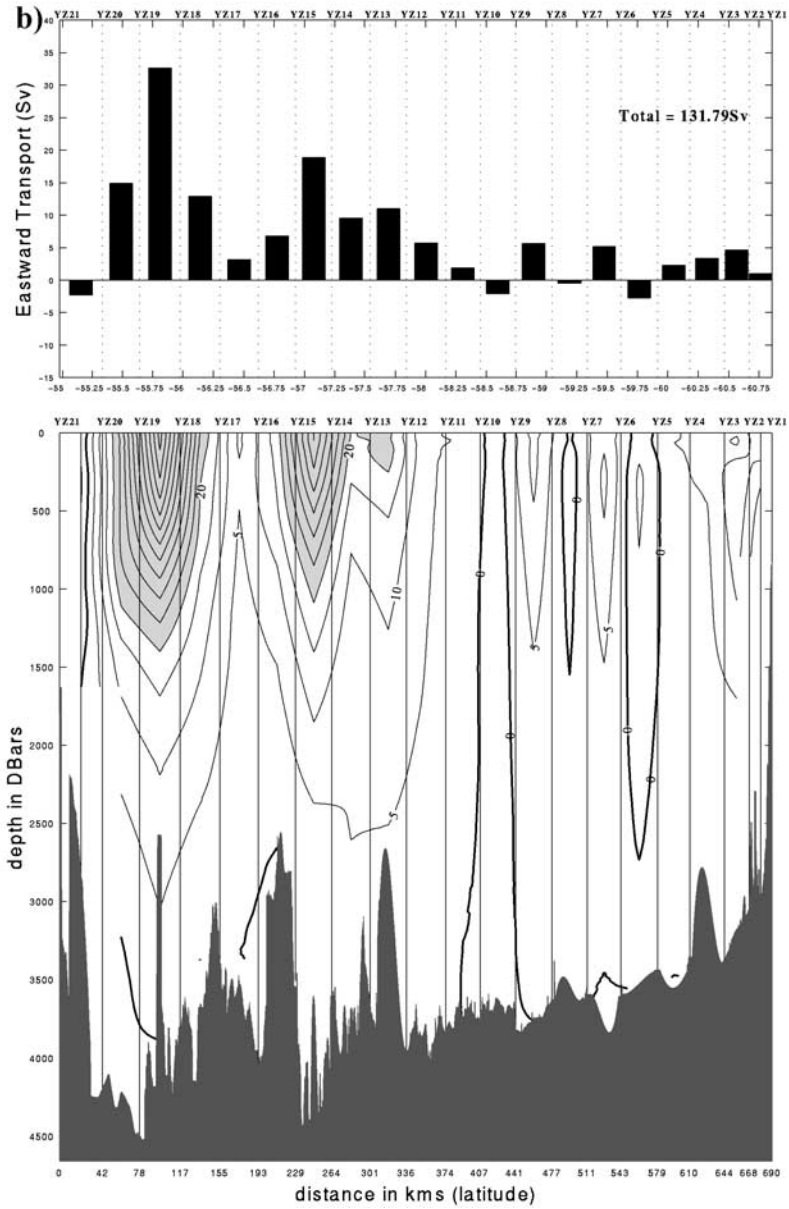

Figure 6. (continued)

somewhat more natural, explanation is that the anomaly was produced by a warm-core anticyclonic eddy, as discussed below.

[21] Figure 9 shows the θ-*S* diagrams of stations YZ2, YZ3, YZ4, and YZ6 corresponding to the Drake 95 data set. Except for the shallowest layers, station YZ6 waters show unambiguously as transitional between YZ2 and YZ3, which suggests that the YZ6 water column was advected from the vicinity of the southern ACC Bdy. In order to confirm this we explored the availability of remote sensing information contemporary to Drake 95. The Arctic and Antarctic Research Center (AARC) group from the University of California, San Diego, kindly screened for us all available NOAA/AVHRR images covering the Scotia Sea in February 1995 and selected the (few) reasonably cloud-free images, which we further processed. Figure 10 shows a NOAA 12 infrared image acquired on 14 February 1995 at 1006 UT, i.e., roughly at the start of the Drake 95 cruise (no further cloud-free images were available later on during the cruise). The image displays intense mesoscale activity of the PF featuring the ''classical'' development of a cyclonic ring at 57°S, 61°W. An eddy feature can also be traced roughly at 59.5°S, 57°W. The core of this eddy is warm with respect to waters found at its periphery, which indicates that the flow is anticyclonic, and the eddy diameter measured in the north-south direction is about 70 nm. The eddy is embedded in colder water from the southern Antarctic Zone and may have entrained some cold water from near the southern ACC Bdy on its periphery, which would account for the thin cold margin found north of the eddy. The limb of the eddy can be discerned to the north, to the west, and to the south. To the east, however, the clouds partially mask the eddy, so the easternmost extent of the feature cannot be properly discerned. Some of the post-

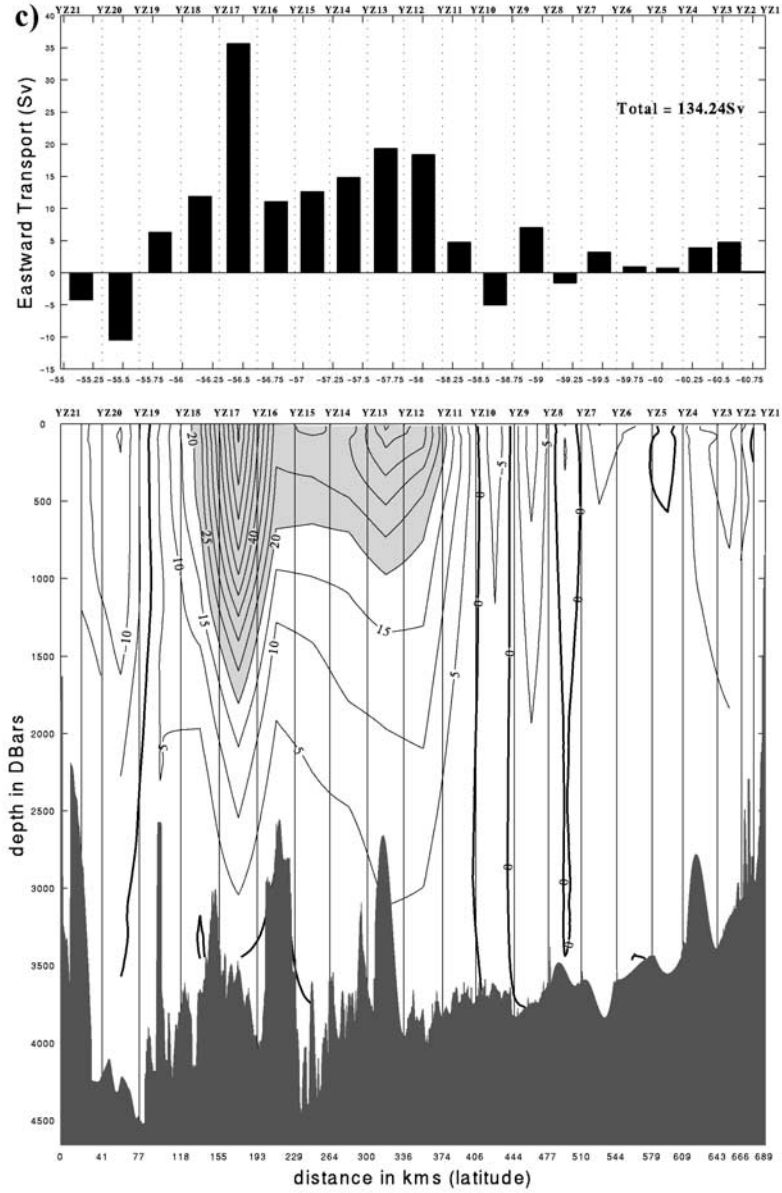

Figure 6. (continued)

cruise cloud-free images (not shown here) suggest that the eddy may have shifted eastward after 14 February. In any case it is clear that if the eddy was advected eastward (or rather southeastward), a section across it would look very much like our SR1b hydrographic distributions between stationsYZ2 and YZ6 (see Figures 2a and 3a). Note that the ADCP data also support the idea of anticyclonic flow between 59.8°S and the southern edge of the YZ2–YZ6 anomalous band (Figure 8). Of course, the eddy might have extended sufficiently eastward that it was "felt" at the SR1b section even with little or no eastward advection. On the basis of all this evidence we conclude that the hydrographic discontinuity observed between stations YZ2 and YZ6 during Drake 95 was related to a deep-reaching anticyclonic eddy. Furthermore, we believe that all similar features observed during the other occupations of the SR1b section were of the same nature.

[22] *Meredith et al.* [1996] reported on data from bottom pressure recorders deployed along the SR1b section. Their Multi-Year Return Tide Level Equipment (MYRTLE) recorder was deployed at 59.7°S, and its records showed very different characteristics from those obtained at their SD2 mooring at 60.8°S. The MYRTLE records displayed much larger amplitude changes in pressure, by a factor of 2 or more, than those of the SD2 gauge, and they exhibited low coherence values with the SD2 fluctuations at periods over 5 days. *Meredith et al.* [1996, p. 22,492] associated this fact with the "apparently anomalous eddy-like feature with continental water properties" described by *King and Alderson* [1994] and concluded that [*Meredith et al.*, 1996, p. 22,492] "this feature is a permanent meander in the boundary between the ACC and the Weddell-Scotia Confluence." We do believe that there is such a permanent meander in the area, but it happens west of SR1b. As

Table 1. Contribution of the ACC Frontal and Interfrontal Zones to the Net Geostrophic Transport Across SR1b in Drake 95, Drake 96, and Drake 98[a]

	Drake 95	Drake 96	Drake 98
SAZ	0 (0)	−2 (−2)	−15 (−15)
SAF	44 (44)	60 (60)	65 (65)
PFZ	0 (0)	0 (0)	0 (0)
PF	76 (72)	55 (52)	70 (66)
AZ	13 (9)	7 (6)	9 (6)
Bdy	11 (8)	11 (9)	5 (3)
Total	144 (133)	131 (125)	134 (125)
WSDW	−1	−0.5	−0.7

[a] The classical zonation of the ACC at Drake Passage consisting of four latitudinal bands, Subantarctic Zone (SAZ), Polar Frontal Zone (PFZ), Antarctic Zone (AZ), and Continental Zone (CZ), limited by three frontal areas (SAF, PF, and southern ACC Bdy), has been adopted here. The contribution of the SACCF is included in the AZ budget. The meridional extent of the frontal areas has been subjectively defined by a 5 cm s^{-1} geostrophic velocity threshold at surface. The boundary between the SAF and the PF bands is considered to be at the latitude where the surface geostrophic velocity attains a relative minimum. The transports have been computed using the maximum common depth between adjacent stations as a variable depth reference level. Values in parentheses correspond to alternative transport calculations using the depth of the 0°C isotherm as a zero-motion reference level. The last row indicates transport below the 0°C isotherm relative to that reference level. Units are sverdrups. Positive (negative) values denote an eastward (westward) transport.

Meredith et al. [1996] recall, this feature is persistent enough to show up in atlas maps of contoured dynamic topography [e.g., *Orsi et al.*, 1995]. Moreover, *Challenor et al.*'s [1996] results obtained with *Semtner and Chervin*'s [1992] Parallel Ocean Climate Model (POCM) display a convincing *S*-folding of the surface flow in the Antarctic Zone, east of the model's bathymetric feature representing the Shackleton Fracture Zone and west of SR1b. The Shackleton Fracture Zone extends across the ACC in the NW–SE direction between the South Shetlands shelf and 58.5°S, northwest of Elephant Island (see Figures 1 and 10). In the AVHRR image shown in Figure 10, an S-shaped hydrographic structure is seen crossing the Shackleton Fracture Zone at 59°S and about 3° west of the anticyclonic eddy observed at 59.5°S, 57°W. A careful scrutiny of the image suggests that the flow is cyclonic between that S-shaped feature and the anticyclonic eddy and that there is interaction between these cyclonic and anticyclonic structures. A blowup of the POCM output shown by *Challenor et al.* [1996] also suggests the presence of cyclonic circulation on the "lee" side (east) of the Shackleton Fracture Zone.

[23] We are inclined to think that the eddies (or rather the permanent eddy) producing the hydrographic anomalies observed during the *Hespérides* occupations of SR1b are ultimately due to the interaction of the southernmost ACC jets with the Shackleton Fracture Zone (this may be the reason why *Rojas et al.* [1998] did not observe such features on SR1a, which is located west of the fracture zone). Taking the climatological frontal positions given by *Orsi et al.* [1995] into account, the lee of the fracture zone, with the southern ACC Bdy to the south and the SACCF far to the north, may be a rather "dead" area where little forcing exists to push the eddies eastward, which would account for their permanence. Since these eddies are deep-reaching, an additional trapping mechanism in the lee of the fracture zone might be the deep circulation in the region, which is thought to consist of WSDW flowing west from Orkney Passage along the southern boundary of the Scotia Sea [*Nowlin and Zenk*, 1988]. On the other hand, *Moore et al.*'s [1997] maps of constant potential vorticity suggest that these eddies should be able to drift meridionally along 54°–55°W with little dynamical constraint. This could be the reason that the hydrographic anomalies are found at different latitudes in different SR1b occupations.

4.3. Observed ACC Transport Variability

[24] Table 1 shows our estimates of the ACC net geostrophic transport across SR1b in February 1995, 1996, and 1998 and of the contribution of the different ACC frontal and interfrontal zones to the total flow. *Whitworth and Peterson* [1985] reason that the fluctuations in the ACC transport can be reasonably approximated with geostrophic computations. On the other hand, all deep current meter records obtained at Drake Passage in the past provide a clear indication that the ACC velocity should not be considered negligible at any intermediate depth if a realistic ACC transport value is to be assessed. As an example, *Whitworth* [1983] and *Whitworth and Peterson* [1985] calculated year-long averages of the current velocity across Drake Passage at 2500 m depth and obtained an eastward flow above 2 cm s^{-1},

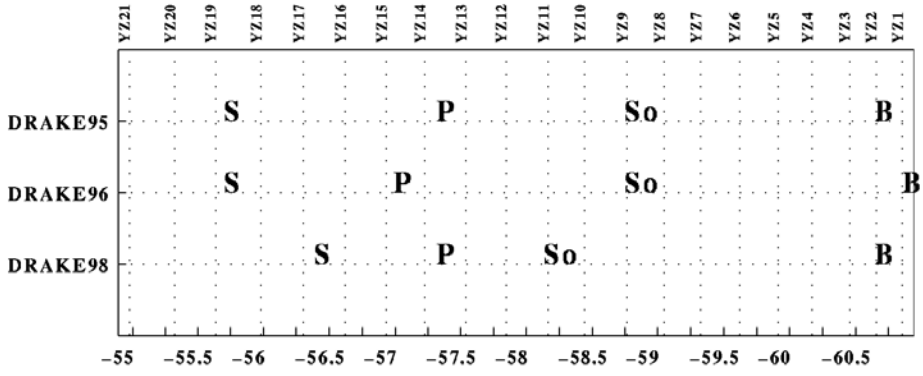

Figure 7. Location of the ACC fronts on SR1b in the Drake 95, Drake 96, and Drake 98 cruises. S, P, So, and B denote the positions of the Subantarctic Front, Polar Front, Southern ACC Front, and southern ACC Boundary, respectively.

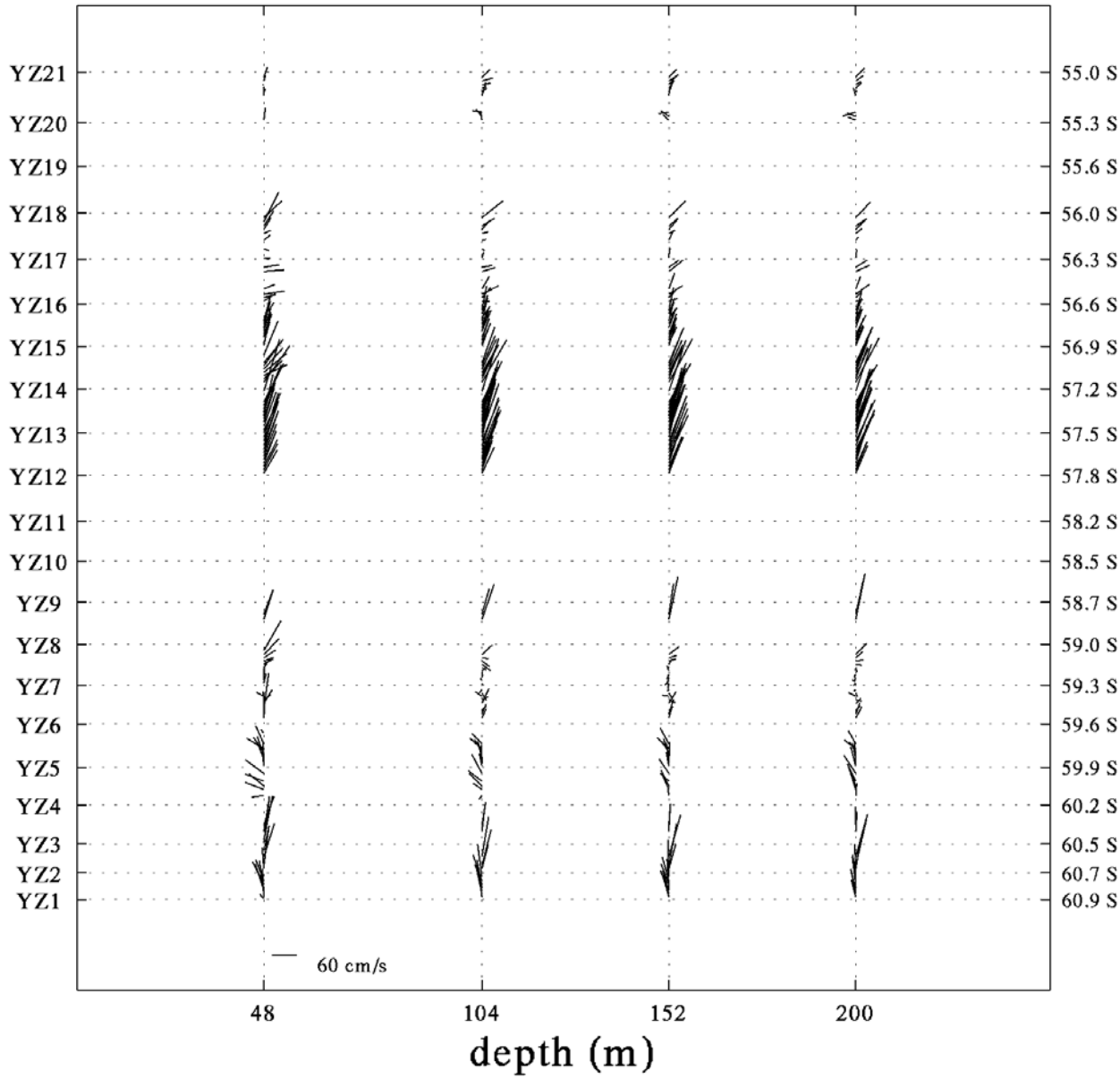

Figure 8. Drake 95 survey. ADCP current velocity distribution on SR1b at 48, 104, 152, and 200 m depth layers. The northward/southward and eastward/westward directions are parallel to the figure margins. Blanks are due to the lack of data.

which, if extrapolated to the entire water column as a barotropic contribution, yielded an extra eastward transport of more than 15 Sv with respect to the transport obtained under the assumption that the flow is zero at 2500 m (even after they removed a deep westward baroclinic contribution below 2500 m computed with respect to the 2500 m depth level, they still obtained a net additional eastward transport of about 10 Sv). This is the main reason why we decided to compute the ACC transports using the maximum common depth between adjacent stations as a variable depth reference level. An additional reason was the quality of our ADCP data sets: there were large stretches of SR1b for which we were not able to obtain good quality ADCP data during Drake 96 and Drake 98 because of losses of the DGPS signal onboard.

[25] We did not isolate the contribution of the SACCF to the ACC transport in Table 1 and instead included it in the Antarctic Zone budget (it was difficult to define the northern and southern boundaries of the SACCF jet in the geostrophic current distributions using the same velocity threshold criterion applied to define the other ACC jets). Nevertheless, if we consider that the SACCF transport was at most equal to the transport assigned to the Antarctic Zone band, we may conclude that the contribution of the SACCF jet to the total ACC transport is on the order of 10 Sv, i.e., comparable to the computed contribution of the southern ACC Bdy jet. In fact, we may have slightly overestimated the transport in the southern ACC Bdy band because we did not take into account any deep westward flow below the reference layer in our calculations. The presence of this deep counterflow

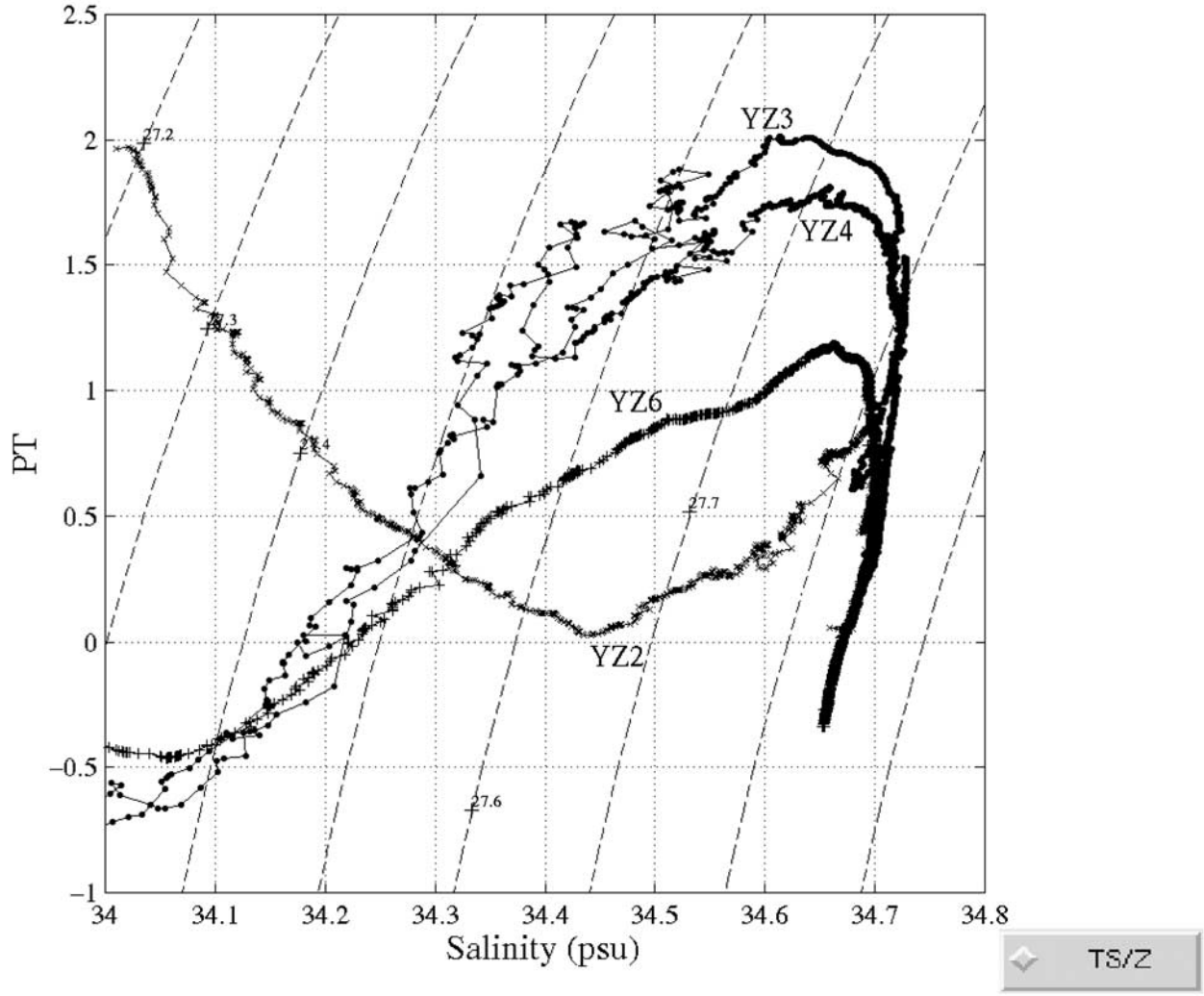

Figure 9. The θ-*S* diagram of stations YZ2, YZ3, YZ4, and YZ6 in Drake 95.

has been documented by the ISOS deep current meter data on the South Shetlands slope [*Nowlin and Zenk*, 1988]. It is also suggested by the bottom water hydrographic properties on the southern half of SR1b upon comparison with values given in the literature for the Weddell Sea deep outflow (not shown).

[26] The net geostrophic transports across SR1b computed for Drake 95, Drake 96, and Drake 98 with respect to the maximum common depth between adjacent stations are 144, 131, and 134 Sv, respectively. Given the large amount of evidence for deep westward flow of WSDW at the southern Drake Passage, we have performed additional transport calculations using the depth of the 0°C isotherm (which is assumed to be the upper limit of the WSDW layer) as the reference level. The results, which are indicated in brackets in Table 1, show a net ACC transport that is lower than the previous estimates by about 7–10 Sv. On the other hand, the transport below the 0°C isotherm is estimated to be between −0.5 and −1 Sv (Table 1). This value is substantially lower than the westward baroclinic transport of −7 Sv computed by *Whitworth* [1983] at Drake Passage owing to the fact that he used a 2500 m reference level (which is shallower than the depth of the 0°C isotherm).

[27] The SAF and PF jets together provide an eastward transport that equals 83% of the net ACC transport across SR1b in Drake 95, 87% in Drake 96, and 100% in Drake 98. The share of each of these two frontal jets also varies from one occupation to another. In February 1995 the PF was the dominant ACC band transporting 76 Sv (i.e., 53% of the ACC net geostrophic transport), whereas the SAF jet contributed 44 Sv (31%) only. In contrast, the SAF jet was the dominant ACC jet in February 1996 (60 Sv, or 46% of the total ACC transport), while the PF played a slightly lesser role in terms of transport rates (55 Sv, 42%). The situation changed again in February 1998: the PF jet was transporting 70 Sv, and the SAF jet was transporting 65 Sv. It is interesting to note that the SAF was located 40 nm farther south in Drake 98 than in Drake 96, but this was not reflected by any significant change in the associated transport. Furthermore, this southward displacement of the SAF was accompanied by the presence of a significant westward geostrophic transport (15 Sv) in the stretch of Subantarctic Zone intersected by SR1b, which resulted in the fact that the ACC net geostrophic

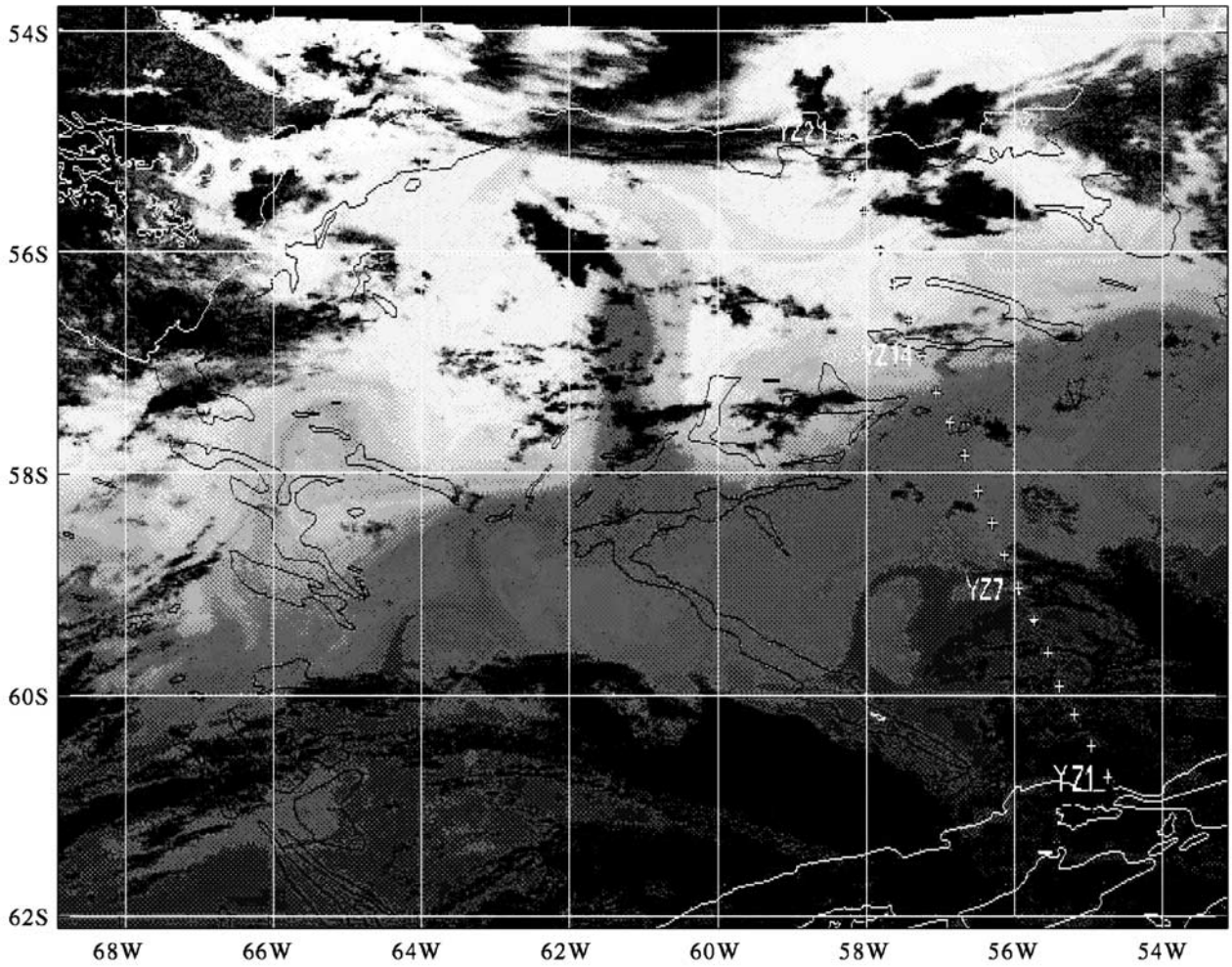

Figure 10. AVHRR image of the Scotia Sea acquired by NOAA 12 on 14 February 1995 at 1006 UT. Red colors mean relatively warm waters, and blue colors mean relatively cold waters. Clouds are masked in black. The coastline and the 1000 m bathymetric contour are indicated by thin white lines, and the 3000 m contour is indicated by a black line. The SR1b stations are marked with crosses. See color version of this figure at back of this issue.

transport was almost the same as in February 1996 despite an increase in the PF jet transport of 15 Sv. *Whitworth* [1983] observed in 1979 that whenever the SAF shifted to the south, additional warm water from the Pacific was drawn into the northern Drake Passage, but the net transport showed no increase because a high ridge located approximately at 57°S, 67°W, upstream of the ISOS current meter array, caused incoming Pacific water to recirculate around it. Similarly, on the SR1b section, which is some 300 nm east of the ISOS Drake Passage transect, the band of westward flow observed north of the SAF in February 1998 is likely due to anticyclonic recirculation occurring south of Burdwood Bank. Indeed, this is what is suggested by the θ-*S* diagram of the relevant stations (not shown here).

[28] The paradigm that the variability of the ACC net geostrophic transport is mainly in the barotropic field has provided a strong foundation for assessing the temporal variability of the transport through Drake Passage on the basis of bottom pressure differences across the passage [e.g., *Whitworth and Peterson*, 1985; *Meredith et al.*, 1996]. However, these methods should be used in conjunction with either altimetry data or field measurements to provide insight into the way in which the ACC transport is split into different zonal bands.

5. Concluding Remarks

[29] R/V *Hespérides* performed WOCE-type repeated surveys of the SR1b section across the Scotia Sea in February 1995, 1996, and 1998. The results of the *Hespérides* cruises illustrate a four-front structure of the ACC (the SAF, the PF, the SACCF, and the southern ACC Bdy), each of these fronts having an associated baroclinic jet. The fronts changed latitude, width, and intensity from one occupation to the next. The observed changes in the ACC transport between consecutive occupations was strongly influenced by the undersampled mesoscale temporal variability of the ACC system.

[30] The initially planned WOCE SR1a line was substituted by SR1b so as to overlap optimally a track of the

ERS-1 and 2 satellites. Our results suggest that this decision may have had an unforeseen cost: introducing additional mesoscale variability in the hydrographic fields in the southern part of the Antarctic Zone, related to the presence of the the Shackleton Fracture Zone. This may become a problem for the WOCE synthesis given the scales of the processes that are of interest to the World Climate Research Program's (WCRP's) world experiment. The Climate Variability and Predictability (CLIVAR) Initial Implementation Plan [*WCRP*, 1997] envisages a continuation of repeated choke point measurements on SR1 under the umbrella of the CLIVAR component on climate fluctuations at decadal to centennial timescales (CLIVAR/DecCen). We suggest that whether the choke point section should go back to the original Drake Passage SR1a line so as to reduce the "mesoscale noise" in the hydrographic distributions should be carefully considered. Additionally, we strongly recommend that monthly XBT surveys keep being performed on the choke point section year-round in order to distinguish better the mesoscale and subseasonal variability from the interannual and decadal changes in the ACC structure.

[31] **Acknowledgments.** The authors wish to thank Oswaldo López, M. Pilar Rojas, Fernando Hermosilla, Xavier Gironella, Pedro A. Arnau, M. Dolores Herrera, Angélica M. de León, Luc Vandenbulcke, Damià Gomis, Susanna Pla, Beatriz López, José Escánez, Antoni Calafat, Albert Palanques, Pere Puig, Mario Manríquez, Pedro Jornet, Pablo Rodríguez, Fernando Uceta, Miguel Pancorbo, Angel Cristóbal, Elisabet Almela, Arturo Castellón, Zacarías García, and other members of the Drake 95, Drake 96, and Drake 98 scientific crews who helped in various ways to obtain the data sets used in this paper. We are equally grateful to Robert Millard Jr., who provided guidance for CTD data postprocessing work, complying with WOCE standards, and to Ljiljana Simic, who also assisted in data postprocessing. We deeply acknowledge the expert support of the crew of R/V *Hespérides* during the cruises. We are especially thankful to Guillermo Sánchez and Manuel Velarde for their unbelievable repair work of the lower plate of *Hespérides*' Rosette in Drake 95. We also want to thank Robert Kluckholm and the Antarctic Support Associates team in Punta Arenas for their valuable help in February 1995 and UCSD's AARC for screening and providing us with NOAA/AVHRR imagery. Two anonymous reviewers provided extremely detailed and constructive reviews of the paper. Their suggestions have greatly helped us improve the original manuscript. We wish to express our gratitude to them. This work has been partially funded by the Spanish Comisión Interministerial de Ciencia y Tecnología, grants AMB94-0436, AMB94-1253-E, ANT95-1718-E, and ANT96-0866. Ileana Bladé was funded by the Spanish Ministerio de Educación y Ciencia and by the Comissionat d'Universitats i Recerca of the Generalitat de Catalunya.

References

Callahan, J. E., The structure and circulation of deep water in the Antarctic, *Deep Sea Res.*, *19*, 563–575, 1972.

Carpenter, J. H., The Chesapeake Bay Institute technique for the Winkler dissolved oxygen method, *Limnol. Oceanogr.*, *10*, 141–143, 1965.

Challenor, P. G., J. F. Read, R. T. Pollard, and R. T. Tokmakian, Measuring surface currents in Drake Passage from altimetry and hydrography, *J. Phys. Oceanogr.*, *16*, 2748–2759, 1996.

Deacon, G. E. R., A general account of the hydrology of the South Atlantic Ocean, *Discovery Rep.*, *15*, 1–24, 1933.

Deacon, G. E. R., Physical and biological zonation in the Southern Ocean, *Deep Sea Res., Part A*, *29*, 1–15, 1982.

García, M. A., BIO Hespérides covered WOCE SR1b in February 1995, *Int. WOCE Newsl.*, *23*, 33–35, 1996.

García, M. A., O. López, J. Puigdefàbregas, and J. Sospedra, Repeated observations of the ACC on WOCE SR1b, *Int. WOCE Newsl.*, *29*, 16–18, 1997.

Joyce, T. M., On in situ calibration of shipboard ADCPs, *J. Atmos. Oceanic Technol.*, *6*, 169–172, 1989.

King, B., and S. Alderson, SR1 repeat hydrography/ADCP, Drake Passage, November 1993, *Int. WOCE Newsl.*, *15*, 13–15, 1994.

Meredith, M. P., J. M. Vassie, K. J. Heywood, and R. Spencer, On the temporal variability of the transport through Drake Passage, *J. Geophys. Res.*, *101*, 22,485–22,494, 1996.

Moore, J. K., M. R. Abbott, and J. G. Richman, Variability in the location of the Antarctic Polar Front (90°–20°W) from satellite sea surface temperature data, *J. Geophys. Res.*, *102*, 27,825–27,833, 1997.

Nowlin, W. D., Jr., and M. Clifford, The kinematic and thermohaline zonation of the Antarctic Circumpolar Current at Drake Passage, *J. Mar. Res.*, *40*, 481–507, 1982.

Nowlin, W. D., Jr., and W. Zenk, Westward bottom currents along the margin of the South Shetland Island Arc, *Deep Sea Res., Part A*, *35*, 269–301, 1988.

Nowlin, W. D., Jr., T. Whitworth III, and R. D. Pillsbury, Structure and transport of the Antarctic Circumpolar Current at Drake Passage from short-term measurements, *J. Phys. Oceanogr.*, *7*, 778–802, 1977.

Orsi, A. H., T. Whitworth III, and W. D. Nowlin Jr., On the meridional extent and fronts of the Antarctic Circumpolar Current, *Deep Sea Res., Part I*, *42*, 641–673, 1995.

Peterson, R. G., and L. Stramma, Upper-level circulation in the South Atlantic, *Prog. Oceanogr.*, *26*, 1–73, 1991.

Pollard, R., and J. Read, A method for calibrating shipmounted acoustic Doppler profilers and the limitations of Gyro compasses, *J. Atmos. Oceanic Technol.*, *6*, 859–865, 1989.

Reid, J. L., and R. J. Lynn, On the influence of the Norwegian-Greenland and Weddell Seas upon the bottom waters of the Indian and Pacific Oceans, *Deep Sea Res.*, *18*, 1063–1088, 1971.

Rojas, R., Y. Guerrero, T. Calvete, and W. García, WHP repeated hydrography section SR1, Drake Passage, *Int. WOCE Newsl.*, *32*, 38–40, 1998.

Semtner, A. J., and R. M. Chervin, Ocean general circulation from a global eddy-resolving model, *J. Geophys. Res.*, *97*, 5493–5550, 1992.

Smith, W., and D. Sandwell, Global sea floor topography from satellite altimetry and ship depth soundings, *Science*, *277*, 1956–1962, 1997.

Sprintall, J., R. Peterson, and D. Roemmich, High resolution XBT/XCTD measurements across Drake Passage, *Int. WOCE Newsl.*, *29*, 18–19, 1997.

Whitledge, T. E., S. C. Malloy, C. J. Patton, and C. D. Wirick, Automated nutrient analysis in seawater, *Rep. BNL-51398*, Brookhaven Natl. Lab., Natl. Tech. Inf. Serv., Springfield, N. Y., 1981.

Whitworth, T., III, Zonation and geostrophic flow of the Antarctic Circumpolar Current at Drake Passage, *Deep Sea Res., Part A*, *27*, 497–507, 1980.

Whitworth, T., III, Monitoring the transport of the Antarctic Circumpolar Current at Drake Passage, *J. Phys. Oceanogr.*, *13*, 2045–2057, 1983.

Whitworth, T., III, and W. D. Nowlin Jr., Water masses and currents of the Southern Ocean at the Greenwich Meridian, *J. Geophys. Res.*, *92*, 6462–6476, 1987.

Whitworth, T., III, and R. G. Peterson, Volume transport of the Antarctic Circumpolar Current from bottom pressure measurements, *J. Phys. Oceanogr.*, *15*, 810–816, 1985.

World Climate Research Program (WCRP), *CLIVAR Initial Implementation Plan*, Geneva, 1997. (Available through http://www.dkrz.de/clivar/ht.html).

World Meteorological Organization, World Ocean Circulation Experiment Plan, vol. II, Scientific background, *WMO/TD 243*, Geneva, 1988.

World Ocean Circulation Experiment (WOCE), Manual de operaciones WOCE, vol. 3, secc. 3.1, part 3.1.3, Operaciones y Métodos del WOCE (in Spanish), *Informe de la Oficina WHP WHPO 91-1, Informe WOCE N° 68/91, Rev. 1*, WOCE Int. Proj. Off., Southampton Oceanogr. Cent., Southampton, U. K., 1998.

I. Bladé, J. Puigdefàbregas, and J. Sospedra, Laboratori d'Enginyeria Marítima, E.T.S. d'Enginyers de Camins, Canals i Ports, Universitat Politècnica de Catalunya, c/Jordi Girona 1-3, mòdul D1, 08034 Barcelona, Spain.

A. Cruzado and Z. Velásquez, Centre d'Estudis Avançats de Blanes, Consejo Superior de Investigaciones Científicas, Camí de Sta. Bàrbara s/n, 17300 Blanes (Girona), Spain.

H. García, Scripps Institution of Oceanography, University of California, San Diego, 9500 Gilman Drive, La Jolla, CA 92093–0244, USA.

M. A. García, Direcció General de Ports i Transports, Generalitat de Catalunya, Av. Josep Tarradellas 2-6, 08029 Barcelona, Spain. (mgarlop@ciccp.es; wmagarcia@correu.gencat.es)

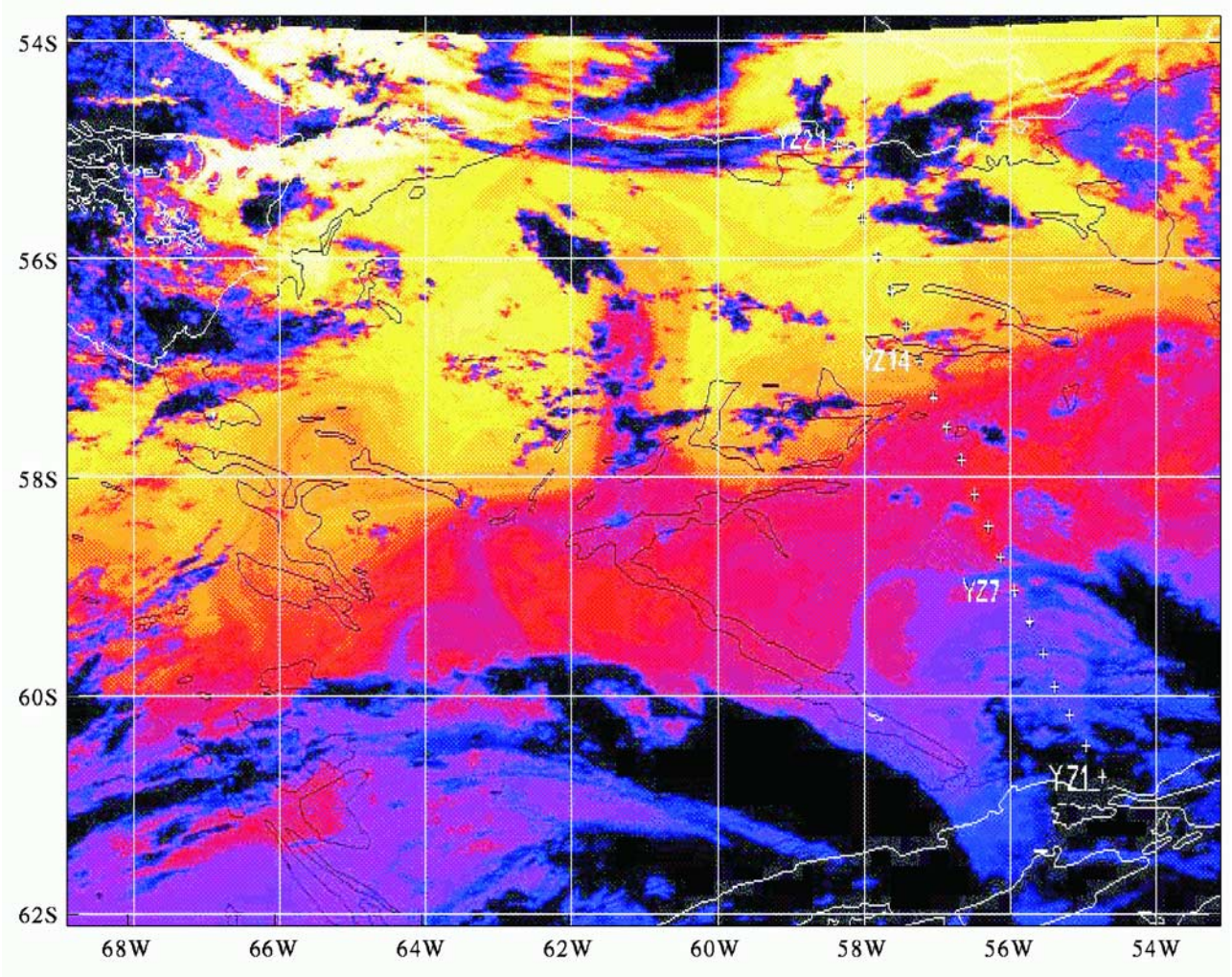

Figure 10. AVHRR image of the Scotia Sea acquired by NOAA 12 on 14 February 1995 at 1006 UT. Red colors mean relatively warm waters, and blue colors mean relatively cold waters. Clouds are masked in black. The coastline and the 1000 m bathymetric contour are indicated by thin white lines, and the 3000 m contour is indicated by a black line. The SR1b stations are marked with crosses.